

THESIS

COMPUTATIONAL INVESTIGATION OF BIOLOGICAL DOSE-VOLUME OUTCOME
PREDICTORS IN 29 CANINE NASAL TUMOR PATIENTS TREATED WITH
STEREOTACTIC RADIATION THERAPY

Submitted by

Rafe McBeth

Department of Environmental and Radiological Health Sciences

In partial fulfillment of the requirements

For the Degree of Master of Science

Colorado State University

Fort Collins, Colorado

Summer 2012

Master's Committee

Advisor: Dongqing Zhang

Susan LaRue

James Custis

Asa Ben-Hur

ABSTRACT

COMPUTATIONAL INVESTIGATION OF BIOLOGICAL DOSE-VOLUME OUTCOME PREDICTORS IN 29 CANINE NASAL TUMOR PATIENTS TREATED WITH STEREOTACTIC RADIATION THERAPY

The ability to mathematically model biological response to radiation dose in the tumors of cancer patients is a significant goal for the medical physics community. Although much work has been done in this area, novel treatment approaches are challenging the current knowledge of the radiation biology and oncology communities. In particular, doses five to ten times higher than traditional treatments are prescribed in stereotactic radiation therapy. These new treatment techniques are thought to have different mechanisms that cause cell death in comparison to classical treatments. These extraordinarily high doses are made possible by using advanced imaging, treatment planning, linear accelerator capabilities and immobilization to precisely target cancer while sparing healthy normal tissue.

Biologically guided radiation therapy (BGRT) and biologically based treatment planning (BBTP) methods offer the next attractive step forward in radiation therapy. To examine the capabilities of biological based dose parameters, a mature data set of 29 canine nasal tumor patients was analyzed using the generalized equivalent uniform dose (gEUD) and the dose to a relative volume. Over one hundred individual predictors were inspected, with greater than five thousand individual tests, in search of optimal indicators of patient outcome. Testing showed that high negative gEUD values and the minimum dose to the tumor were highly significant predictors in the outcome of the patients. However, more robust techniques need to be added to the analysis in order to validate these results.

TABLE OF CONTENTS

1	INTRODUCTION	1
1.1	Introduction	1
1.2	Equivalent Uniform Dose	3
1.3	Generalized Equivalent Uniform Dose ^[45,35]	3
1.4	Canine Nasal Tumors ^[44]	5
1.5	Goal of this study	6
2	MATERIALS AND METHODS	7
2.1	Patient plan export	7
2.2	Python data analysis program ^[1,30,29,8]	7
2.3	Calculation of the generalized equivalent uniform dose (gEUD)	10
2.4	Calculation of volume doses	11
2.5	Predictor grouping	12
2.6	Clinical inputs	13
2.7	Survival analysis	13
2.8	Multiple testing correction	14
3	RESULTS	15
3.1	Basic analysis	15
3.2	gEUD analysis	16
3.3	Survival Analysis	17
4	DISCUSSION AND CONCLUSIONS	26
4.1	Discussion	26
4.2	Future Work	29
4.3	Conclusion	29

CHAPTER 1

INTRODUCTION

1.1 Introduction

Radiation Therapy is a vital component in the treatment of many cancers. Recent technological advances have lead to exciting new treatment modalities and protocols. At Colorado State University's Veterinary Teaching Hospital and many human radiation oncology departments, stereotactic radiation therapy (SRT) or stereotactic body radiation therapy (SBRT) is being used to deliver ablative doses of radiation with sub-millimeter accuracy^[42,33,37,4,28]. SRT has many advantages over classical treatment protocols: a theoretical biological advantage from an increased dose per fraction, fewer patient visits due to accelerated treatment protocol, a reduction in treatment costs and a more effective use of resources^[28]. Hypofractionated treatment protocols and SRT take principles from Conventional Radiation Therapy (CRT), Three Dimensional Conformal Radiation Therapy (3D-CRT), Intensity Modulated Radiation Therapy (IMRT), Image Guided Radiation Therapy (IGRT) and expand upon them to create a more advantageous treatment modality.

Initially stereotactic radiation therapy (SRT) was used to treat brain tumors and was defined as stereotactic radiosurgery (SRS)^[3,39,15]. Treatments often consisted of a single large dose and were administered using a collection of focused radioactive isotopes. The radiobiological rationale for SRT is that a few large dose fractions, in a relatively short overall treatment time, result in a more potent biological effect^[42]. SRS, SBRT and SRT treatments have been shown to be effective in many publications spanning several decades, confirming their usefulness in the treatment of benign and malignant lesions^[39,3,15]. Advancements in linear accelerator technology have resulted in the capability to deliver the same high doses of radiation as seen with previous radiosurgery approaches.

The use of computed tomography (CT) allows for accurate structure delineation and

treatment planning. CT scans also allow for the estimation of the dose to the patient by performing Monte Carlo based dose calculations. The density of the various tissues or Hounsfield units are used to estimate the ability of the x-ray to penetrate the tissue along the beams path to the tumor/target volume. Multi-leaf collimators are used to shape the radiation beam to the tumor in all dimensions by using information from preliminary CT scans. By using multi-leaf collimators (MLC), linear accelerators can form a thin narrow strip of radiation and scan across the tumor, while varying the exposure time. This technique, known as intensity modulation, allows the clinician to preferentially target dose to the tumor volume. Using on board imaging and novel immobilization devices, current linear accelerators are able to accurately setup patients, which minimized the planned target volume (PTV) and reduced the normal tissue toxicity^[20].

In addition to the technological advantages, hypofractionated protocols are more convenient for the patient and a more cost-effective treatment modality than traditional radiation therapy^[4]. While traditional radiation therapy techniques, CRT and IMRT, strive for homogeneous dose distributions, heterogeneity within the target is increased with SRT treatments and is considered acceptable for targets not involving normal tissue^[33]. In addition, although hypoxic subregions in solid tumors may not be stable, it has been hypothesized that hotspots within the central region of a tumor might offer a special advantage in killing radioresistant hypoxic cells^[4].

Much work has been done on mathematical models of dose response to tumors and normal tissues and their application to treatment planning and treatment evaluation^[31,7? ,35]. The linear-quadratic model, the most commonly used model for cell survival, has become widely debated due to its over prediction of cell killing when applied to large dose per fraction treatments such as SRT^[32,6,36]. Alternatives have been offered to account for this difference, such as the universal survival curve^[36], but have not become widely accepted. Two other models that have been used extensively to model tumor control are the equivalent uniform dose (EUD)^[34] or generalized equivalent uniform dose (gEUD)^[35] and tumor control proba-

bility (TCP). In relation to SBRT treatment it has been suggested that EUD is the preferred indicator for prospective description due to its insensitivity to estimates of radiosensitivity and tumor volume^[27]. Due to this fact, the generalized equivalent uniform dose will be the focus of this investigation.

1.2 Equivalent Uniform Dose

The concept of Equivalent Uniform Dose was introduced by Niemierko^[34] and is defined as the biologically equivalent dose that, if given uniformly, would lead to the same cell kill in the tumor volume as the actual nonuniform dose distribution. The original definition of EUD was based on the mechanistic linear quadratic cell survival model described above. EUD can be calculated using the following equation:

$$EUD = 2 \text{ Gy} \cdot \frac{\ln \left[\frac{1}{V} \sum_{i=1}^N V_i (SF_2)^{D_i/2 \text{ Gy}} \right]}{\ln(SF_2)}, \quad (1.1)$$

where V is total volume, V_i is the volume of the i th subvolume within the dose-volume histogram (DVH), D_i is the dose to the i th subvolume, and SF_2 is the surviving fraction after 2 Gy. The equivalent uniform dose in this form has been used in various applications^[43,10,27] but the majority of work has been focused on Niemierko's second form of the equivalent uniform dose, the generalized equivalent uniform dose.

1.3 Generalized Equivalent Uniform Dose^[45,35]

Shortly after the original presentation of equivalent uniform dose Niemierko expanded his definition to include both tumors and normal tissues and named it the Generalized Equivalent Uniform Dose (gEUD):

$$gEUD = \left(\frac{1}{V} \sum_i v_i D_i^a \right)^{\frac{1}{a}}, \quad (1.2)$$

where V is total volume, V_i is the volume of the i th subvolume within the dose-volume histogram (DVH), D_i is the dose to the i th subvolume, and a is a dimensionless variable parameter. The equation is an applied version of a well known mathematical function called the generalized mean. The gEUD has the property that as $a \rightarrow \infty$, the gEUD approaches the maximum dose to the volume of interest and as $a \rightarrow -\infty$, the gEUD approaches the minimal dose. For $a = 1$, the gEUD is equal to the arithmetic mean, and for $a = 0$, it is equal to the geometric mean. The arithmetic mean or simply the average is defined as the sum of the number divided by the total number of elements. In contrast, the geometric mean is often used to normalize the ranges being averaged, preventing over weighting of the average for any range of values. The geometric mean is calculated by taking the n th root of the products of the n values of interest.

While maintaining the original definition of EUD for tumors, the gEUD represents the uniform dose which leads to the same probability of injury as the corresponding inhomogeneous dose distribution. The parameter a may be determined empirically by fitting with published dose-volume data^[18,14] or with analogous data used in an individual institutional practice. Investigators have extensively studied and used this form of the EUD to both evaluate and optimize plans with very good results^[45,40,12,9,31,41], but are only recently being applied to stereotactic protocols^[11,38].

Another benefit of the gEUD formalism is that it can be connected to the other dose-response models. In his 1999 paper^[35], Niemierko proposed a way to link EUD with the TCP. TCP can be calculated based on gEUD as

$$TCP = \frac{1}{1 + \left(\frac{TCD_{50}}{gEUD}\right)^{4\gamma_{50}}} \quad (1.3)$$

where TCD_{50} is the tumor dose to control 50% of the tumors when the tumor is homogeneously irradiated and γ_{50} is a unitless model parameter that is specific to the tumor of interest.

In a 2007 paper, Gay and Niemierko^[16] stated that gEUD could be extremely useful in validating TCP models in hypofractionated radio-surgery. They believe that large doses per fraction are challenging the current tumor control knowledge based on standard fractionation and clinicians can no longer rely on their acquired clinical intuition based on standard fractions. Accurately validated models could assist the clinician in choosing safer and more effective treatment plans with these cutting edge treatments. The need for such validation has prompted the American Association of Physicist in Medicine (AAPM) to recently release a thorough report on the implementation of biologically guided radiation therapy (BGRT)^[31]. In addition, multi-institutional data sets are being established to further study the issues related to biological dose models^[5].

1.4 Canine Nasal Tumors^[44]

Canine nasal tumors account for approximately 1% of all neoplasms in dogs. Radiation therapy is the treatment modality of choice. On average, dogs with the disease are ten years of age. Environmental components, such as tobacco smoke or fossil fuel combustion products, have been suggested as contributors to the disease. Patients often present with clinical signs of unilateral epistaxis or mucopurulent discharge. Definitive diagnosis is achieved via tissue biopsy in conjunction diagnostic imaging, which is often highly suggestive of disease. Carcinomas account for nearly two thirds of all tumors with sarcomas representing the majority of the remaining types. Treatment is often only possible with radiation therapy due to the locally invasive nature of the disease, making curative surgery nearly impossible. Without treatment, canine patients have a median survival time of 95 days. Historically patients are treated with 41 to 54 Gy in 10 to 18 fractions. Median survival for protocols using CT-based computer treatment planning systems is 10 to 19.7 months. Over the course of treatment, patients typically succumb to local progression of tumor resulting in decreased quality of life. Canine nasal tumor patients used for this study were treated using advanced SRT techniques with dose prescriptions of 30 Gy in 3 fractions of 10 Gy. The median survival

time associated with SRT to these patients is 414 days^[2].

1.5 Goal of this study

While many have used TCP models to evaluate treatment plans, assumptions made about the underlying biology, such as linear quadratic formalism, may not be accurate. The goal of this study was to investigate a simple model, the gEUD, to find new information about the outcome of patients treated with stereotactic radiation therapy. For this study, two predictors were extensively tested to evaluate their ability to connect dose-volume information to treatment outcome. Dose to a percentage of the structure volume, a common clinical parameter, and the generalized equivalent uniform dose were analyzed for the planned tumor volume (PTV) and the gross tumor volume (GTV).

CHAPTER 2

MATERIALS AND METHODS

2.1 Patient plan export

Twenty-Nine canine nasal tumor patients were selected for evaluation in the study. Stereotactic radiation therapy (SRT) treatment protocols were prescribed to all patients in the group with the dose prescription of 10 Gy per fraction for three fractions, for a total of 30 Gy. The dose planning technique for the treatment group was to create homogeneous dose distribution within the tumor. All patient structures were contoured by veterinary radiation oncology residents with the help of a boarded veterinary radiologist and approved by a boarded veterinary radiation oncologist. Patients were planned using the Varian (Eclipse version 8.6) treatment planning software. Cumulative dose and absolute volume information was exported from the dose volume histogram (DVH) within the treatment planning software in 1 cGy data steps. Exported data files contained all structures used for the plan in a standard format, with a significantly reduced but representative example below in Data example 1.

2.2 Python data analysis program^[1,30,29,8]

A Python program was created to search and identify the single most significant predictor of clinical outcome. Python was selected as the programming language due to simple syntax, powerful general nature and its ability for mathematical computations. In combination with a Linux based operating system, Python is capable of controlling other command line programs such as gnuplot (plotting,graphics) and the statistical program R within the programming environment. The desire was to create a single program capable of automatically performing all analysis steps and generating useful output in a variety of formats. The program input included the exported dose-volume information from Eclipse and patient out-

```

Patient Name      : Last, First (254791), ()
Patient ID       : 254791
Date            : 19.03.2012 16:45:35
Type            : Cumulative Dose Volume Histogram
Description      : The cumulative DVH displays the percentage
                  (relative) or volume (absolute) of structures
                  that receive a dose equal to or
                  greater than a given dose.

```

```

Plan: IMRS TX
Prescribed dose [cGy]: 3000.0
% for dose (%): 100.0

```

```

Structure: PTV
Approval Status: Approved
Plan: IMRS TX
Course: C1
Volume [cm]: 40.1
Dose Cover. [%]: 100.0
Sampling Cover. [%]: 100.0
Min Dose [cGy]: 2032.2
Max Dose [cGy]: 3455.0
Mean Dose [cGy]: 3089.7
Modal Dose [cGy]: 3123.7
Median Dose [cGy]: 3100.9
STD [cGy]: 120.4

```

Dose [cGy]	Relative dose [%]	Structure Volume [cm]
0	0	40.0898
500	16.6667	40.0898
1000	33.3333	40.0898
1500	50	40.0898
2000	66.6667	40.0898
2500	83.3333	40.0471
3000	100	32.4803

Data example 1: Example Eclipse exported data file for one patient and one structure. The actual exported patient data contained more than 20 structures with dose steps of 1 cGy totaling 100,000 data lines per patient and a total of over 3 million individual lines of data.

come information in Excel format obtained from the radiation oncologist. A list of patient hospital ID numbers initiates the program and each input file is searched for the desired information. Searches were performed using Python regular expressions to easily find blocks of data within the large (>100,000 line) data files. Functions within the Scipy Python package^[26] were used to read in the clinical Excel formatted information. Patient ID's from the DVH file are used as key values for the creation of a Python dictionary structure. Python dictionaries are a data type capable of storing any other Python object and are well suited for constructing a database style structure within the program. Dictionaries consist of key and value pairs allowing stored data for each patient to be accessed by a common key. Once the regular expressions were defined, a findall command was used to collect all file instances that matched the regular expressions. The output of the findall command contains a list of all found items matching the regular expression. The found output lists were then iterated in order to allocate each found match to the correct location. A second level dictionary was

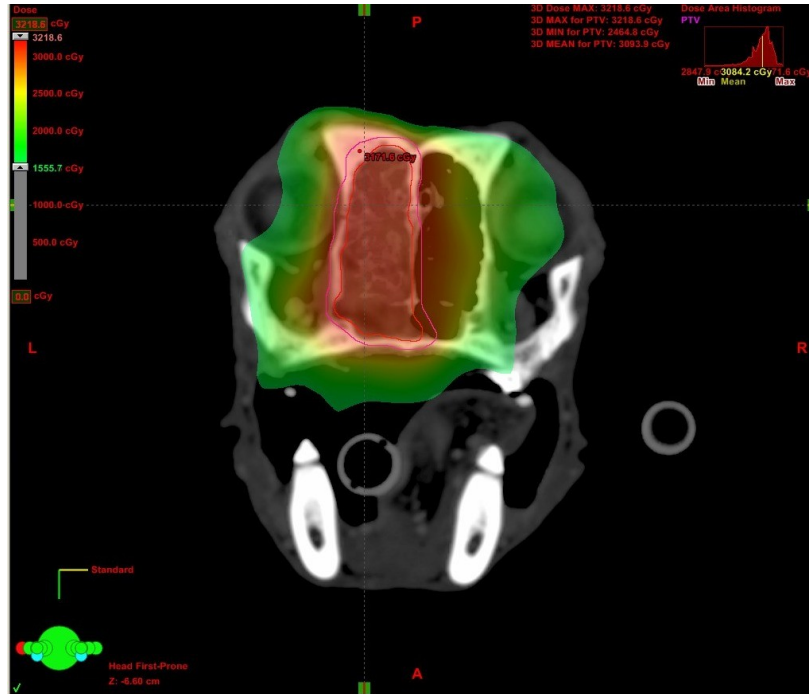


Figure 2.1: Transverse CT slice with representative dose distribution for this group of patients.

created in order to store patient specific data such as the first and last name, plan name and all the structures contained within the plan. Within the Patient structures a third level dictionary was created to store structure specific data such as the raw data, total volume, and minimum dose. A series of Python functions were then created to organize, manipulate and store the desired predictors of the system.

At this stage, the raw input data stored inside the structure dictionary was organized into total dose and absolute volume vectors. The created dose and volume arrays were placed inside the structure dictionaries and auxiliary data files were produced to be used outside the programming environment for collaborative and testing purposes. The relative dose and volume were then computed, stored and used to produce dose volume histograms that would become a part of the program output. Dose volume histograms are used by clinicians during planning and evaluation, allowing for a common reference when viewing new data such as the generalized equivalent uniform dose.

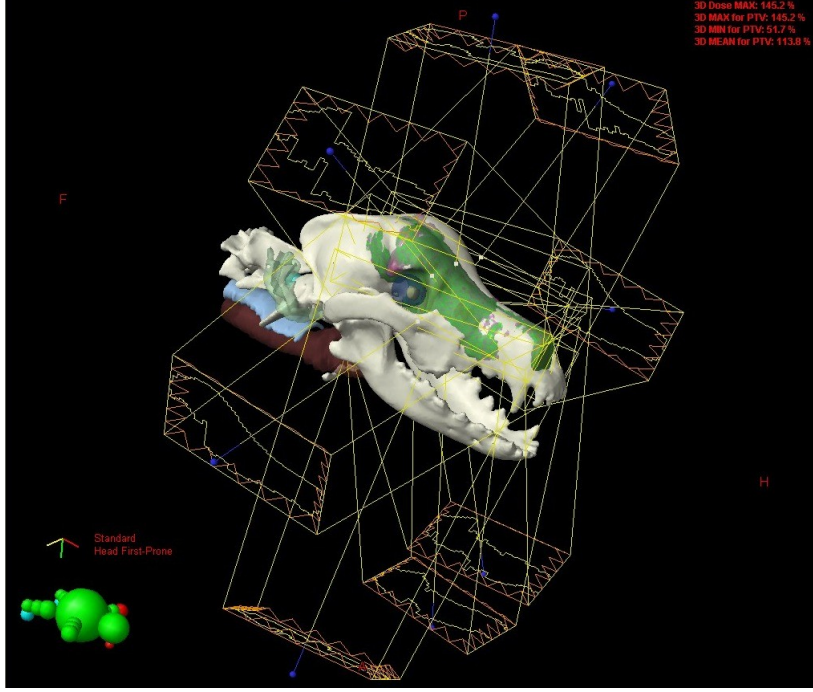


Figure 2.2: Representative radiation beam arrangement for this group of patients.

2.3 Calculation of the generalized equivalent uniform dose (gEUD)

To calculate the gEUD for structures of interest (PTV, GTV), the exported cumulative dose volume histogram had to be converted to a differential dose volume histogram. Conversions were performed using a Python function that takes the dose at each step and adds half the difference between its value and the subsequent value to get the differential dose. The differential volume was calculated as the difference between the subsequent values. The generalized equivalent uniform dose for each patient was calculated using the differential dose-volume values with equation 2.1:

$$gEUD = \frac{1}{V} \left(\sum_{i=1}^N v_i D_i^a \right)^{1/a} . \quad (2.1)$$

Where V is the total volume of the structure, N is the total number of differential dose volume data points, v_i and D_i are the i -th volume and dose point respectively, and a is

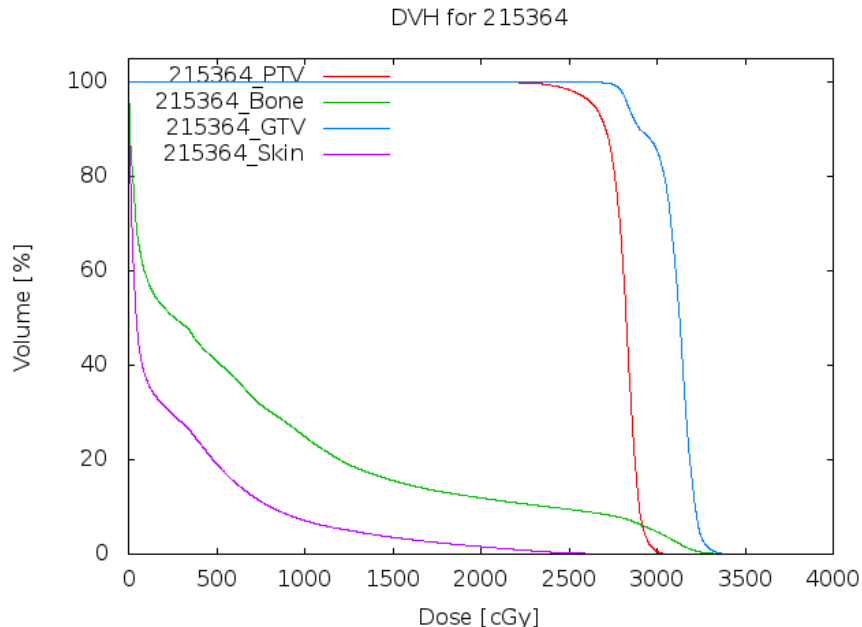


Figure 2.3: Dose volume histogram produced from within the program

the variable parameter that was discussed earlier. To ensure the accuracy of this step, program code and test cases were compared with published data from Gay and Niemieriko, the creator of the gEUD concept^[16]. The resulting gEUD calculations for a from -80 to 50 were placed in the structure dictionary as a two dimensional array (a, gEUD) assuring that a and gEUD values did not get unsorted. Multiple output plots were made to visualize how the gEUD function varies as a function of a . In order to make the analysis more robust, additional common clinical variables, such as dose to a structure percent, were next to enter the program.

2.4 Calculation of volume doses

Common clinical dose prescriptions are given in terms of achieving a prescribed dose to a percent of the volume, often 50%, 90%, 95% or 99%. As a clinically relevant testing predictor the dose to relative volume of 5 to 100 percent, in 5 percent increments was also calculated. To accurately calculate the dose to percent volume a function was created that takes, as

input, the main dictionary, the structure of interest, the percent volume of interest and a epsilon factor. The epsilon value is an error factor used to determine how close to the desired dose is acceptable for calculation. Given the relatively rough scale of output, initial program runs with small epsilon values would return no results for the dose to a specified volume. The final value used for epsilon was set at 1% and results were checked by hand from the Eclipse treatment planning software to verify the accuracy. As with the other created variables in the program, the results were stored into specific dictionary locations.

2.5 Predictor grouping

Each predictor (gEUD values, Dose to percent volume) was scanned amongst all patients to create groupings. The value for an individual predictor was considered as a cutoff point and given a value of zero. All other patient values were compared to this cutoff point, assigned a value of zero if below or equal to the selected cutoff and given a one if the value was above the cutoff. This technique allowed for all possible groupings, based on cut off points, to be assumed for each predictor. The Python function created took the main dictionary, structure of interest and the desired predictor as input. Output produced a separate dictionary containing all the potential groupings for that predictor.

2500	2500 = 0	2500 = 1
2100	2100 = 0	2100 = 0
2400	2400 = 0	2400 = 1
2600	2600 = 1	2600 = 1

Figure 2.4: Patient grouping example showing starting position and two grouping examples. The middle grouping starts with a value of 2500 and compares the rest of the values while the right grouping shows a starting value of 2100.

2.6 Clinical inputs

Clinical inputs were obtained and included the date of treatment, type of tumor, complications, censorship status and survival time. The clinical inputs were contained in excel spreadsheets and imported into the Python programming environment. To insure correct placement, patient ID numbers were used as verification and to place data under the appropriate patient. Survival and censorship status were the only clinical outcome variables of interest for this particular project. Two patients were censored due to an alive status at time of last follow up with survival days being calculated to last follow up. Six patients were censored due to retreatment of the disease, with censorship at the date of retreatment.

2.7 Survival analysis

Statistical analysis was performed by utilizing the rpy2 Python package to access R, an open source and widely used statistical program, within the Python programming environment. A log rank Kaplan Meier survival test^[21] was performed using the survival package in R. The R function took the survival days with censorship and compared them to each grouping of over 200 predictors, a total of 5677 individual tests. Within the function a check was performed to make sure there was at least one quarter of the total patients in each group. Kaplan Meier curves were plotted, saved and the p-value associated with the analysis was extracted back into Python. In order to pick out which predictors and associated cutoff values had the best predictive capability, the output list of two values (predictor and cutoff, p-value) were sorted and predictors that had a p-value of less than 0.05 were output. Checks were also made within the function to handle cases where only one prediction group is given, categorizing the predictor with a p-value of 1 and eliminating it as a possible significant predictor. In addition to the Kaplan Meier survival plots, scatter plots were also created with color coding based on grouping to allow for another visual verification of the results.

2.8 Multiple testing correction

To analyze the uncertainty associated with the results, a simple Bonferroni correction was applied. The Bonferroni modification is a method used to account for multiple comparisons. When multiple comparisons are made, the potential for falsely identifying significance is increased. To account for this, the desired significance level is divided by the number of comparisons to establish the level of significance needed with multiple comparisons. A significance level of 0.01 was desired for this analysis and upon applying the Bonferroni correction to the total number of tests, a modified significance level would be 0.000002.

$$\beta = \frac{\alpha}{n} \approx \frac{0.01}{5700} \approx 0.000002, \quad (2.2)$$

where β is the level of significance needed for multiple comparisons, α is the desired significance level and n is the number of tests performed. Using this level of significance, none of the predictors would achieve the desired significance level. However, many of the groupings were identical and the number of independent tests was much lower than 5700. Further analysis of the groupings, to identify the number of independent tests, would be needed to correctly apply a Bonferroni correction.

CHAPTER 3

RESULTS

3.1 Basic analysis

Twenty-nine patients were analyzed with the program. Basic summary statistics were obtained for all patients in the group and summarized in tables 3.1 and 3.2. It can be seen that for the dose variables used in the planning process, PTV90 and GTV90, there is less variation in the distribution of patient values than in variables such as the PTV min dose and EUD -37. Looking at the plot of the PTV EUD values versus the variable parameter a , fig 3.1, the majority of patients begin very close to the prescribed dose of 30 Gy but begin to disperse as a becomes more negative. This is to be expected as the mean dose is represented by an a value of -1 and the spread shows that dose inhomogeneity is being taken into account by the EUD value. Similarly a GTV EUD vs a plot was generated, fig 3.2, showing a more complex distribution between the patients. From the EUD plots the grouping idea can also be visualized by considering a horizontal line at an a value of interest. Based on the shape of the EUD curve, and choice of cutoff point, the grouping of patients can be visualized.

Table 3.1: General summary statistics for the 29 patients in the study

	Survival (d)	PTV Min dose	PTV EUD-80 (Gy)	PTV EUD-37 (Gy)	PTV 95 (Gy)
Mean	397	18.25	21.40	24.33	27.86
STD	267.1	3.24	3.67	3.91	2.08

Table 3.2: Continued summary statistics for the 29 patients in the study

	PTV 90 (Gy)	GTV 90 (Gy)	GTV 95 (Gy)	GTV 99 (Gy)	PTV Total Vol cm ³	GTV Total Vol cm ³
Mean	29.80	29.84	29.41	28.7	93.48	70.22
STD	1.91	1.78	1.85	2.07	64.47	49.94

3.2 gEUD analysis

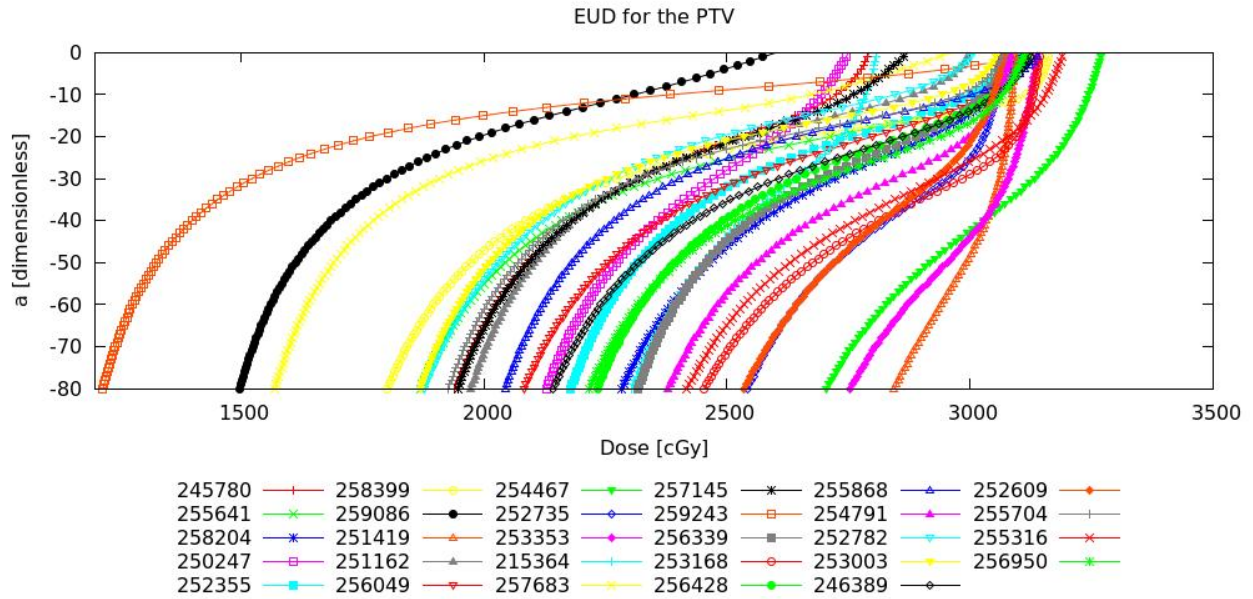


Figure 3.1: Graph of PTV EUD as a function of a . Negative values are highlighted based on the fact that tumors are considered to be defined by negative a values

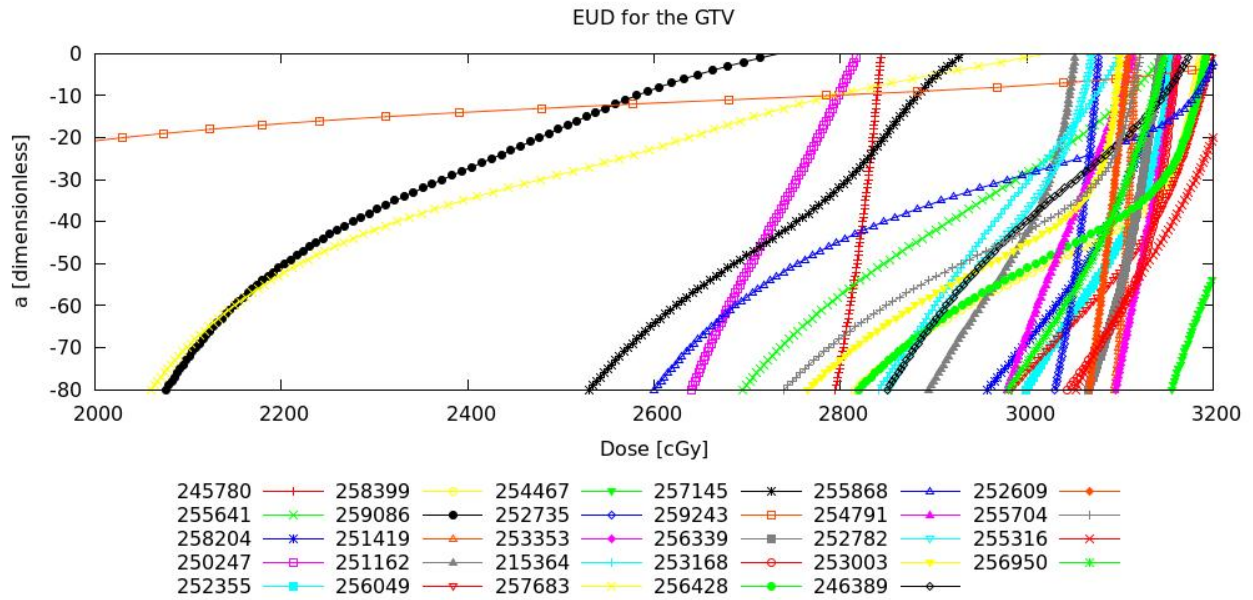


Figure 3.2: Graph of GTV EUD as a function of a . Negative values are highlighted based on the fact that tumors are considered to be defined by negative a values

3.3 Survival Analysis

The Kaplan-Meier based, two group analysis classified multiple highly significant individual predictors of outcome. Six levels of significance were found for a p-value of under 0.01, with multiple predictors per significance level. Multiple predictors were significant at each level due to the same effective groupings being created by the cutoff values. The summary of the analysis is presented in table 3.3, with Kaplan-Meier and scatter plots for each predictor shown in the following figures.

Table 3.3: Results of Kaplan-Meier based, two group analysis

Predictor	Cutoff value (Gy)	p-value	Survival above cutoff
EUD -80	19.26	0.00031	Increased
EUD -37	22.09	0.00031	Increased
Min Dose	16.23	0.00031	Increased
Min Dose	16.64	0.0041	Increased
PTV 10	32.25	0.0073	Decreased
PTV 10	32.40	0.0085	Decreased
GTV 15	32.08	0.0073	Decreased
GTV 15	32.34	0.0085	Decreased

The predictors, EUD-80 with cutoff 19.26 Gy, EUD-37 with cutoff 22.09 Gy and the minimum dose at cutoffs of 16.23 and 16.64 Gy, showed that patients above the cutoff value performed significantly better than patients below the cutoff. However, for dose to 10% of the PTV and dose to 15% of the GTV the results showed that patients below 32.25 Gy and 32.08 Gy performed better than patients above. Although, it is tempting to consider that there is a preferred range of doses, the analysis was performed for individual predictors only and results can not be combined for this particular technique. Analysis with combined predictors could be performed in order to investigate this further.

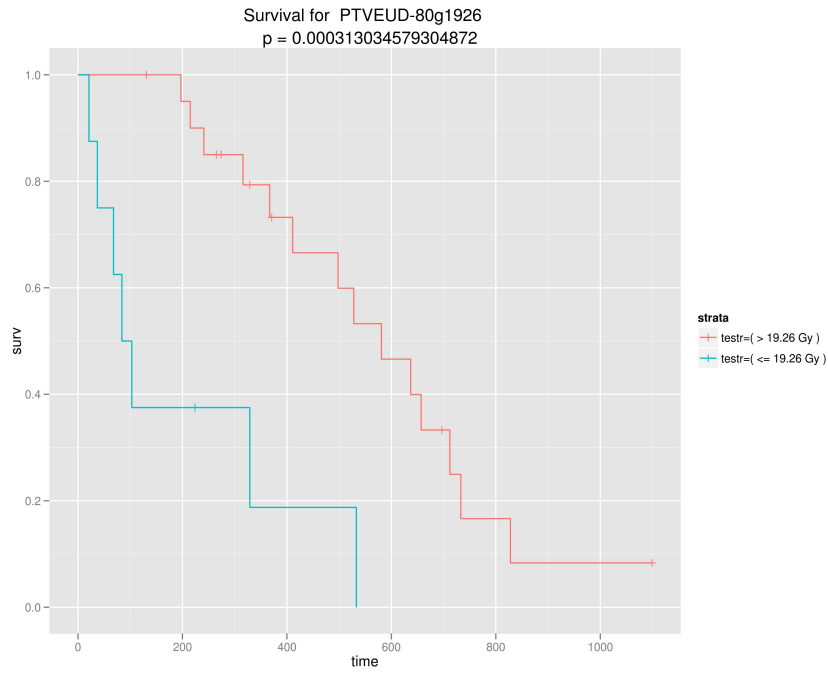


Figure 3.3: Kaplan-Meier two group survival analysis for PTV EUD with a=-80 predictor and cutoff of 19.26 Gy

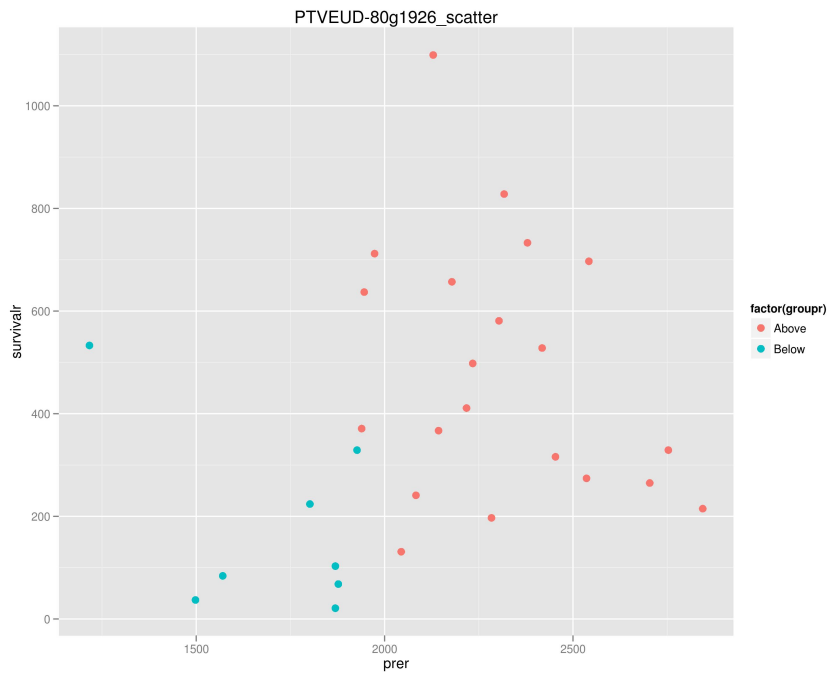


Figure 3.4: Two group scatter plot for PTV EUD with a=-80 predictor and cutoff of 19.26 Gy

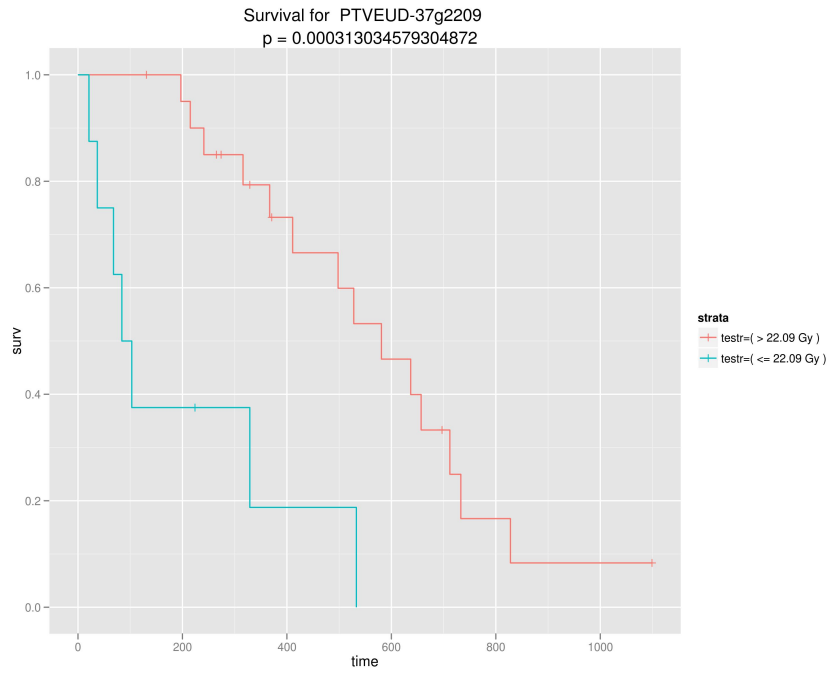


Figure 3.5: Kaplan-Meier two group survival analysis for PTV EUD with a=-37 predictor and cutoff of 22.09 Gy

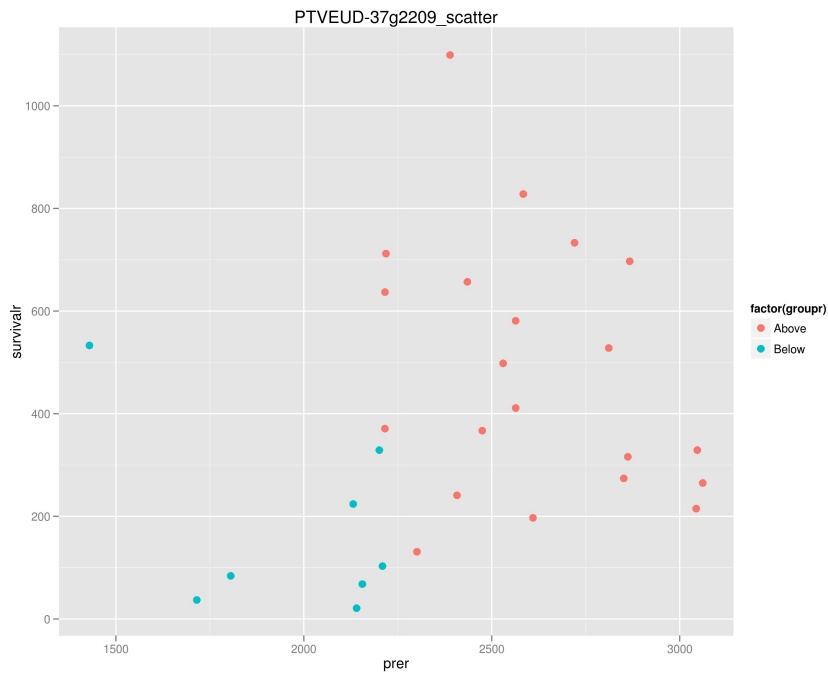


Figure 3.6: Two group scatter plot for PTV EUD with a=-37 predictor and cutoff of 22.09 Gy

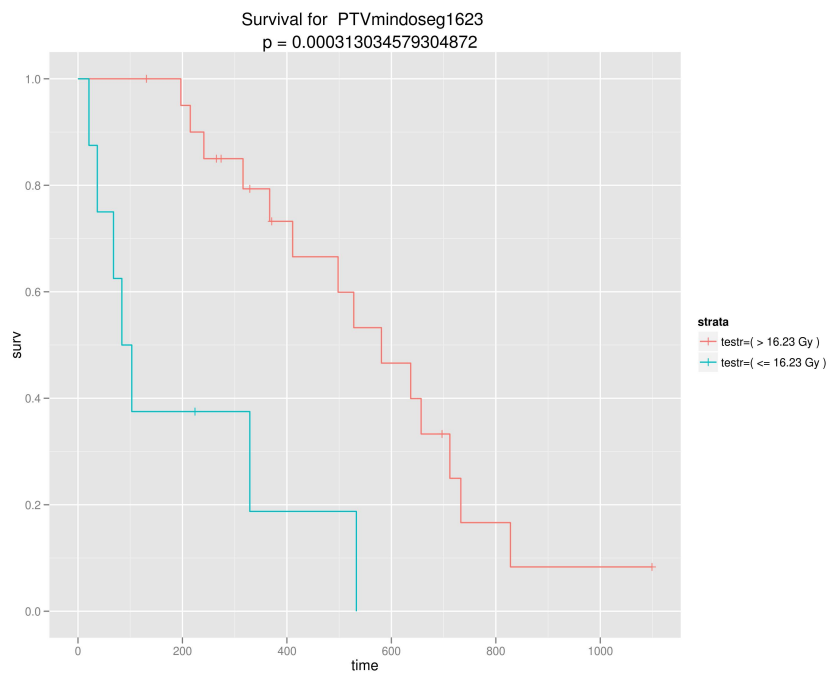


Figure 3.7: Kaplan-Meier two group survival analysis for PTV minimum dose predictor and cutoff of 22.09 Gy

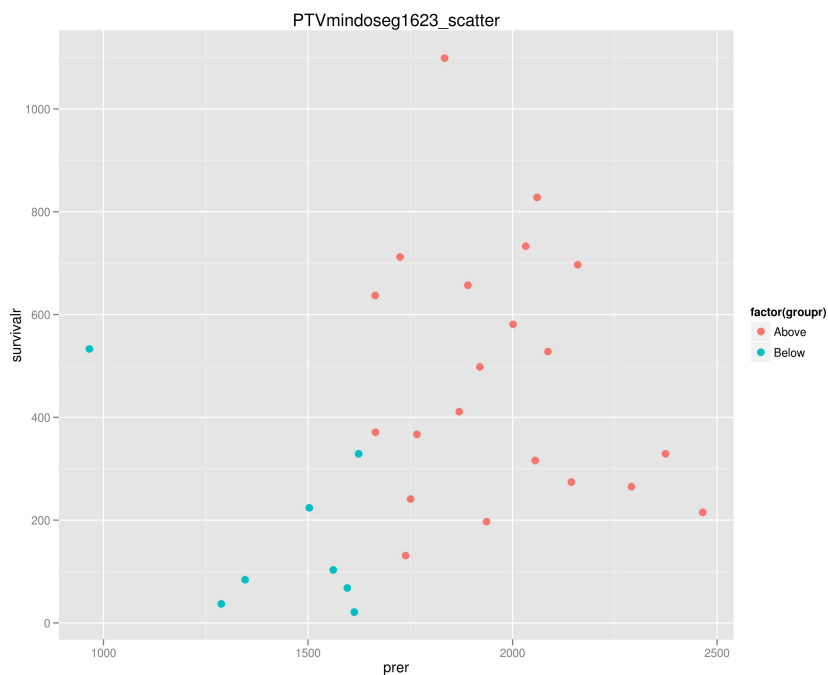


Figure 3.8: Two group scatter plot for PTV minimum dose predictor and cutoff of 16.23 Gy

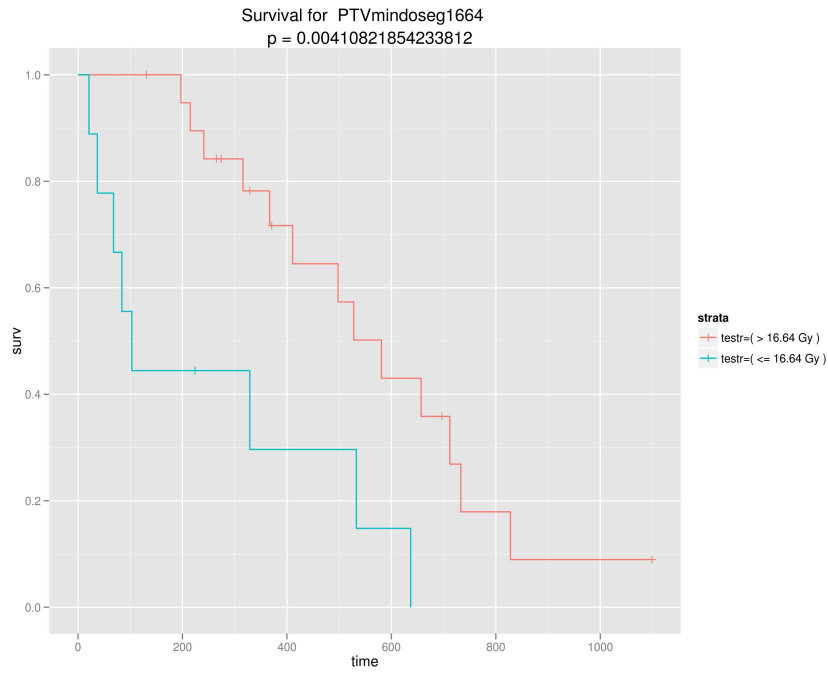


Figure 3.9: Kaplan-Meier two group survival analysis for PTV minimum dose predictor and cutoff of 16.64 Gy

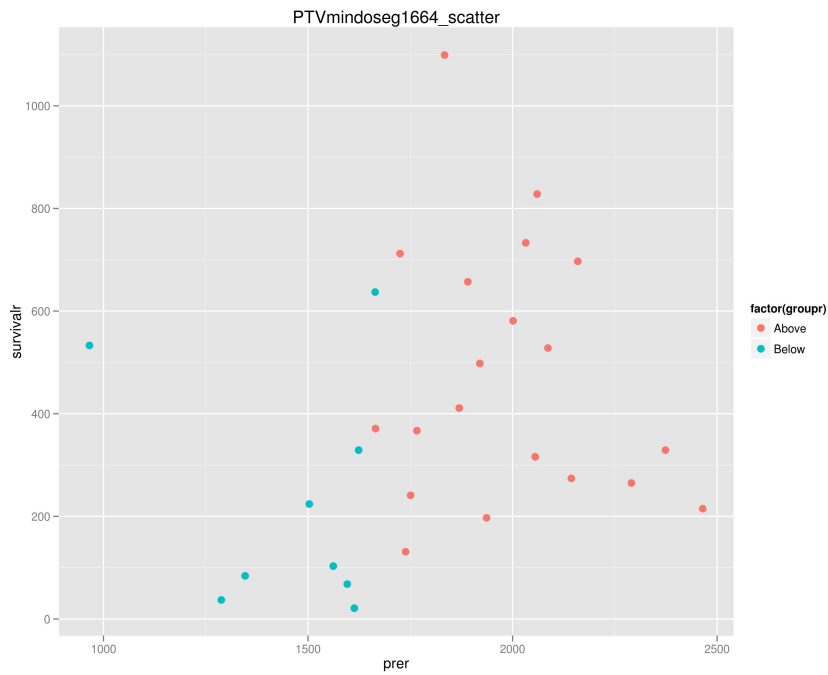


Figure 3.10: Two group scatter plot for PTV minimum dose predictor and cutoff of 16.64 Gy

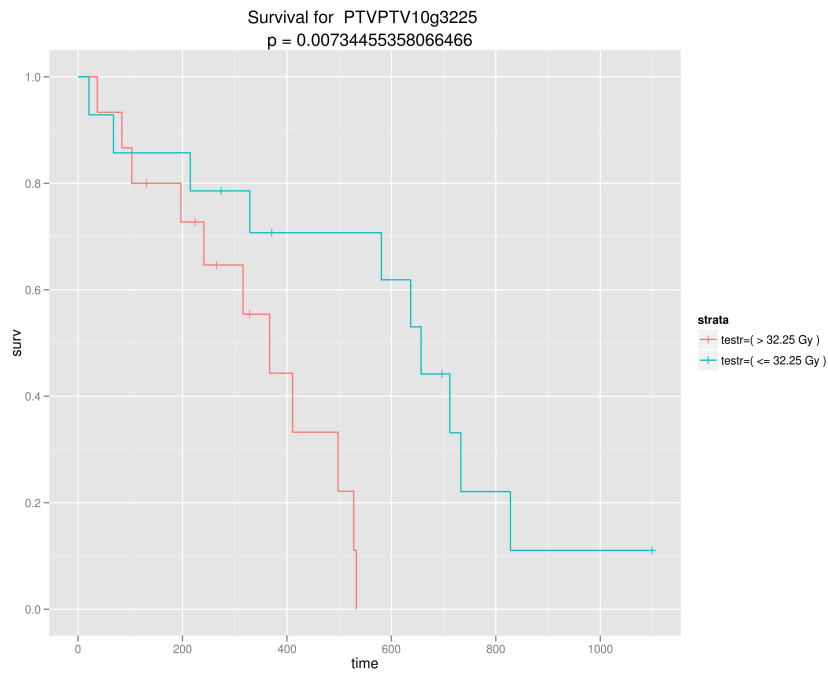


Figure 3.11: Kaplan-Meier two group survival analysis for dose to 10% of the PTV predictor and cutoff of 32.25 Gy

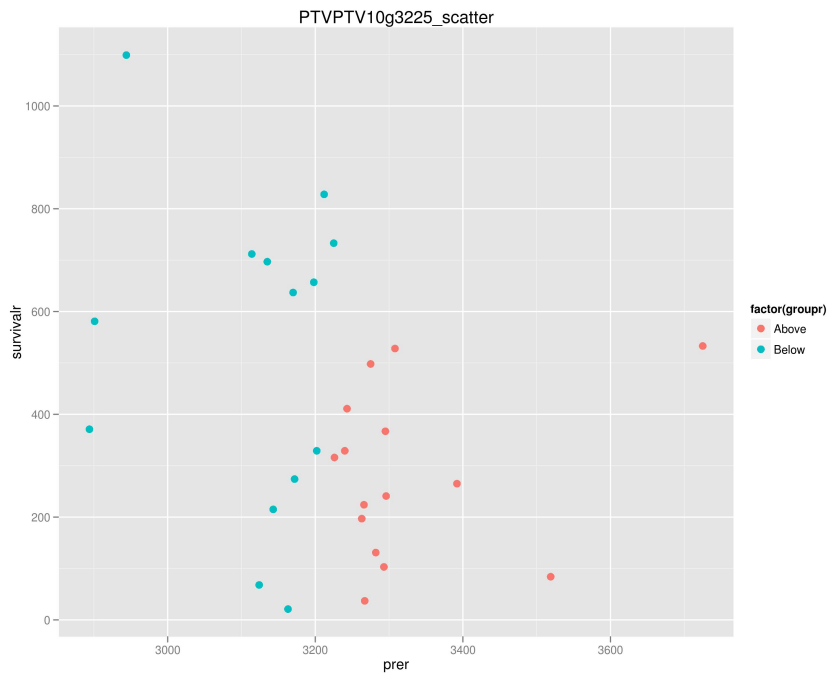


Figure 3.12: Two group scatter plot for 10% of the PTV predictor and cutoff of 32.25 Gy

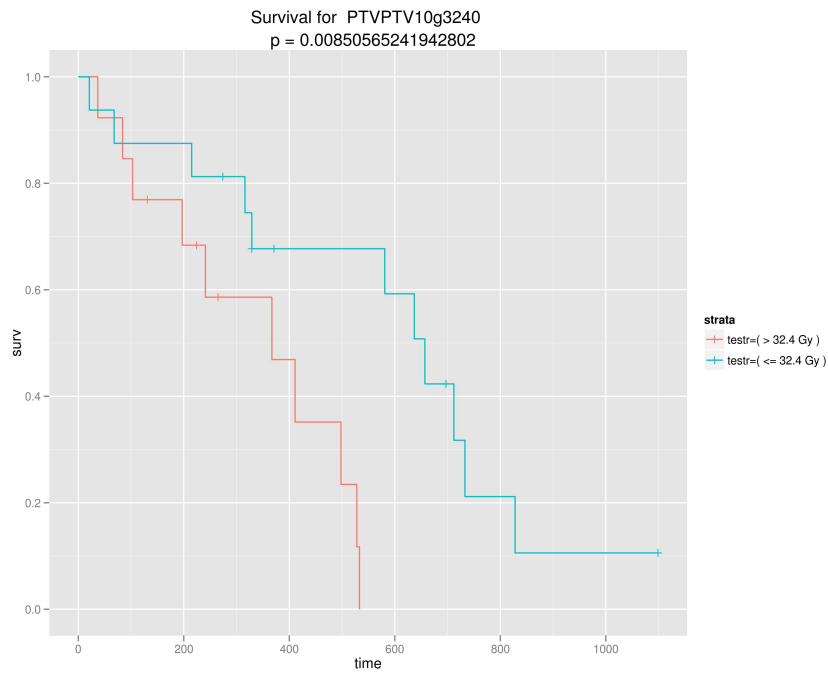


Figure 3.13: Kaplan-Meier two group survival analysis for dose to 10% of the PTV predictor and cutoff of 32.40 Gy

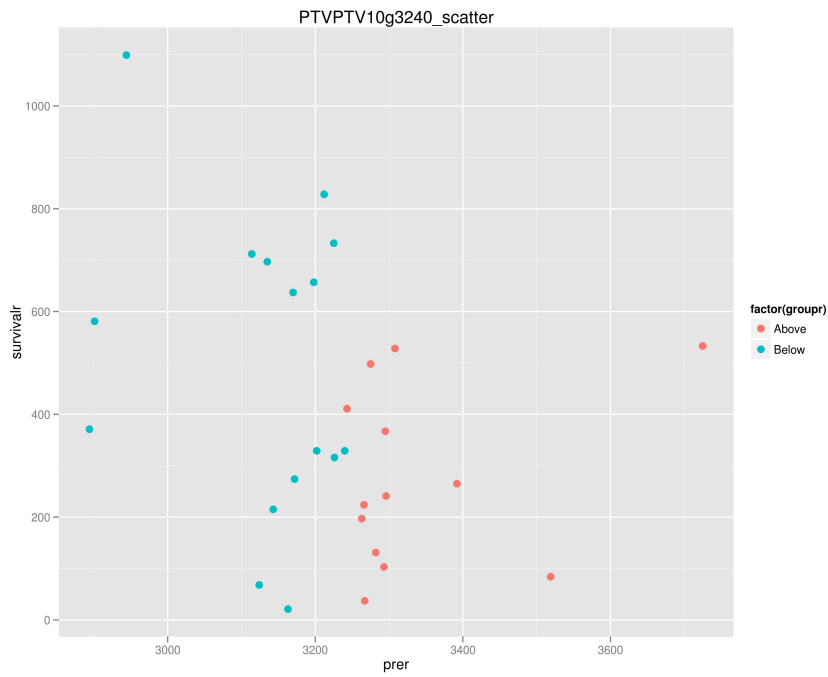


Figure 3.14: Two group scatter plot for 10% of the PTV predictor and cutoff of 32.40 Gy

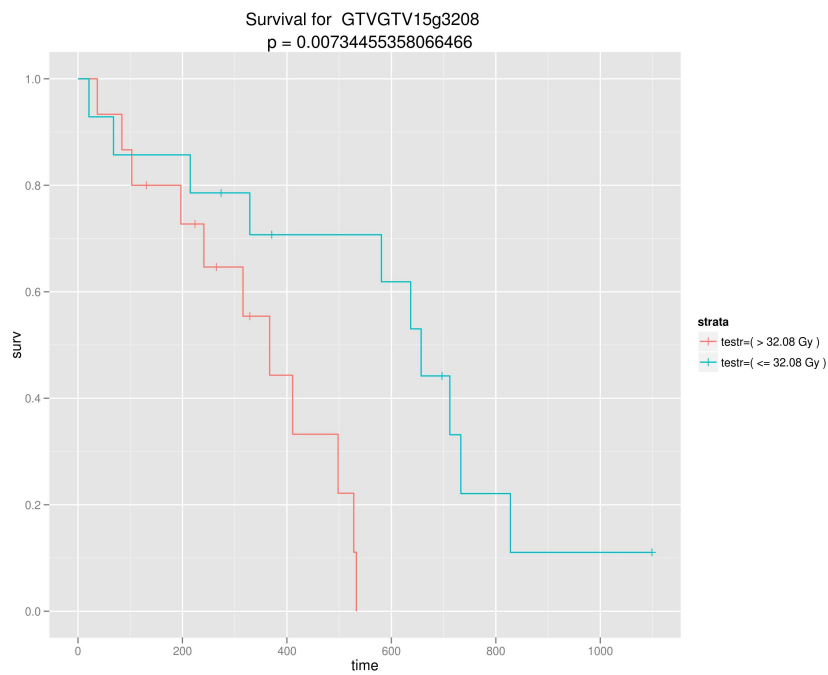


Figure 3.15: Kaplan-Meier two group survival analysis for dose to 15% of the GTV predictor and cutoff of 32.08 Gy

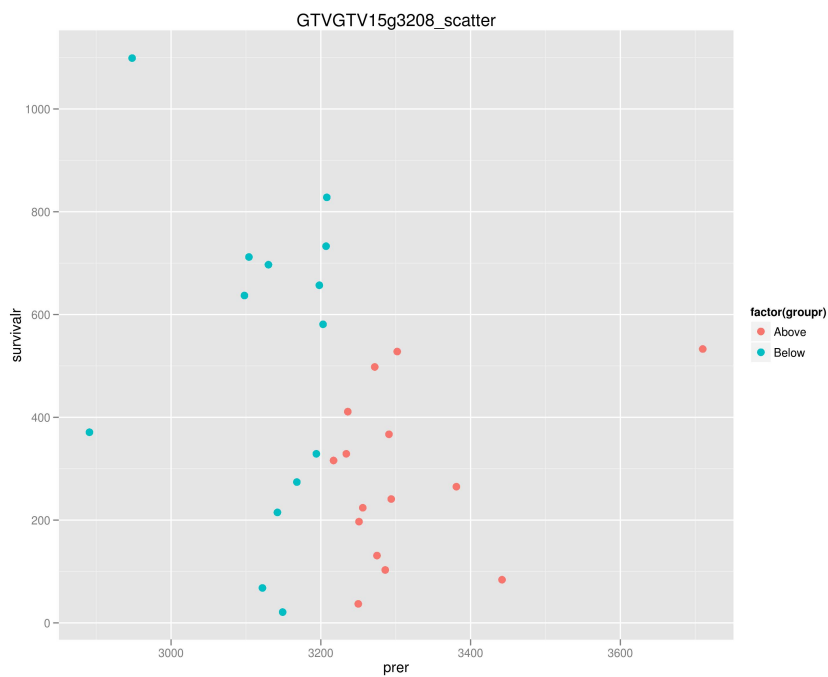


Figure 3.16: Two group scatter plot for 15% of the GTV predictor and cutoff of 32.08 Gy

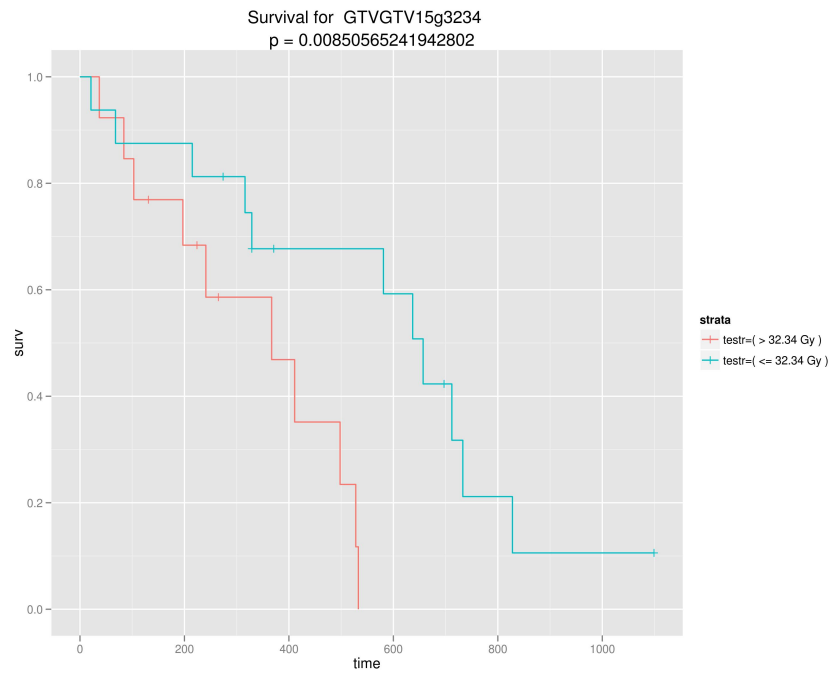


Figure 3.17: Kaplan-Meier two group survival analysis for dose to 15% of the GTV predictor and cutoff of 32.34 Gy

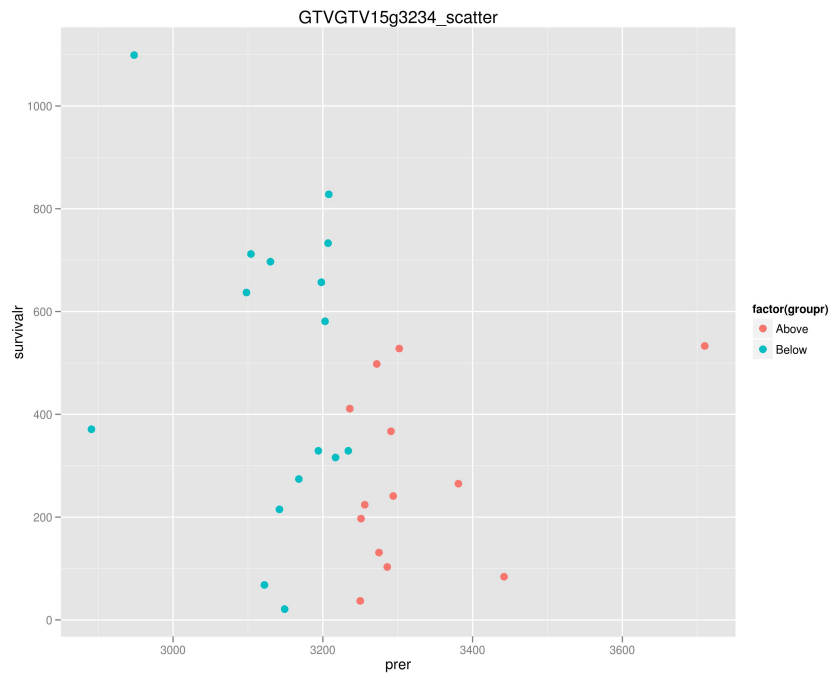


Figure 3.18: Two group scatter plot for 15% of the GTV predictor and cutoff of 32.34 Gy

CHAPTER 4

DISCUSSION AND CONCLUSIONS

4.1 Discussion

The analysis was able to present significant predictors of clinical outcome for canine nasal tumor patients. The dose-volume based predictors highlighted were able to identify specific significant groupings but in themselves are not good predictors of outcome. In addition, a single grouping can be assigned multiple interpretations based upon the predictor to which it is applied. For example, using a gEUD predictor with an a value of -80 implies that the near minimum dose to the PTV is of importance while an a value of -37 corresponds to an assignment of average dose weighted away from the minimum and corresponds to a specific dose volume weighting relationship. The most significant grouping applied to these different predictors can lead to different clinical suggested actions, such as achieving greater than 16.23 Gy minimum dose to the tumor, each justifiable if analyzed individually.

The plot of the gEUD versus a for the PTV explains why a range of a values showed significance. GEUD values held consistent groupings after certain thresholds, such as $a = -50$ in figure 4.1 below. Studies have described a values of around -50 as being very effective in the optimization of the dose distribution to tumors, while using an a value of -20 to describe aggressive tumor types^[41]. Others have used smaller negative values of the parameter a ($-2 \rightarrow -10$) to describe the dose to the PTV^[45]. However, this analysis shows that assigning a concrete a value is difficult and dependent on the non-uniformity of the treatment plan for each patient.

Looking at figure 4.1, the dose distribution to the PTV of patients 245780 and 259086 can be described as having more non-uniformity than other patients in the study. This non-uniformity is highlighted by the variation in gEUD value as a is varied. For example, in the range between $a = -20$ and $a = -10$ the value of the gEUD varies from approximately

17 Gy to 26 Gy. The gEUD model has the ability to classify the non-uniformity across a structure by weighting different ranges of dose more or less dependent of the value of a . Structures that have great dose variation over their volume will have gEUD plots that are highly dependent on a because the gEUD will change greatly as different regions of the dose distribution are weighted more. In contrast, a highly uniform dose distribution should have little variation of the gEUD over different values of a as weighting different ranges will change the value of the gEUD little. A representative uniform dose distribution in this study would be patient 251419 in figure 4.1.

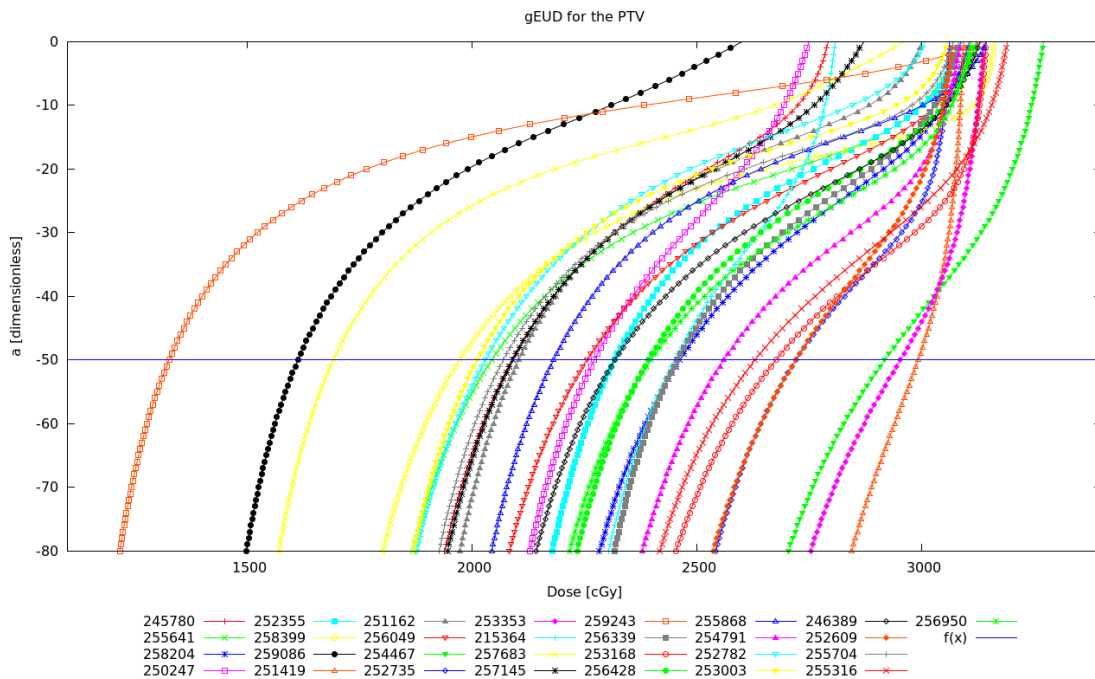


Figure 4.1: gEUD vs a plot showing the groupings created at a values below $a = -50$. The groupings stay consistent for the majority of patients with only a few patients shuffling their order.

The minimum dose and gEUD with large negative a values make intuitive sense based on clinical experience. Patients may survive longer due to increased dose to the PTV resulting in a higher probability of tumor cell killing. In contrast, the ten percent dose to the PTV and fifteen percent dose to the GTV were unexpected significant predictors. Patients that received increased dose had a shorter survival than patients that received a lower dose. A

possible explanation of the ten percent dose to the PTV could be that normal tissues may be included in the volume and an increased dose could lead to normal tissue complications around the tumor. Explanations for the the dose to fifteen percent of the GTV is difficult to justify and more work will need to be done to investigate its potential clinical implications.

Analysis of uncertainty for this technique is also of concern. Without an estimation on the error of the computed p-values it is hard to justify their worth. If applied correctly the Bonferroni modification could allow the current data to stay significant after taking into consideration multiple comparisons. However, there would have to be only thirty-one independent groupings for the highest significance grouping to stay significant. The Bonferroni correction would be changed to

$$\beta = \frac{\alpha}{n} \approx \frac{0.01}{31} \approx 0.00032, \quad (4.1)$$

where β is the level of significance needed for multiple comparisons, α is the desired significance level and n is the number of tests performed. Further analysis would need to be conducted in order to determine if there are truly only thirty-one independent tests. Bootstrapping, a computer-intensive method used to estimate the error in a calculation, is based on resampling, and would be another good candidate for the estimation^[24,13]. Data used within a calculation, such as survival or predictor value, could be randomly resampled with replacement many times (10,000 or more). The original calculation could then be performed with this resampled data to obtain a distribution for the outcome values. The advantage of using bootstrapping techniques to calculate error is that assumptions about the distribution of data, such as normality, do not need to be made in order to validate the analysis.

Another potential improvement on the analysis would be to evaluate the ability of a predictor to classify good versus bad outcome without taking the cutoff value into consideration. Time dependent survival receiver operating characteristic curves (ROC(t)) could be used as the main search function as opposed to the two Kaplan-Meier tests presented^[22]. ROC(t)

analysis can be performed using the survivalROC package for R from within the python environment to a clinically relevant time point, such as one year^[23]. To quantitatively determine if the predictor was useful, the area underneath the ROC(t) curve could be used. Area underneath the ROC curve measures the probability that the predictor being analyzed will accurately classify a favorable versus unfavorable outcome and can be connected to the Wilcoxon statistic^[19].

4.2 Future Work

Future work will include the analysis of additional canine nasal tumor patients treated with the same dose prescription but modified dose distribution. Patients in the second group were treated with simultaneous integrated boosts (SIB) to the center of the tumor. Adding in the second group of patients could help to identify if predictors such as PTV10 and GTV15 have any clinical significance, as patients were given higher dose to smaller volumes corresponding to these regions on the dose volume histogram. The program will also be expanded to include more robust techniques that were found in the literature. Techniques such as the Genetic algorithms used in Gayou's EUCLID outcome analysis tool^[17], or Bayesian network and support vector machine models used to predict two year survival by Jayasurya^[25], can be integrated into the current program.

4.3 Conclusion

In conclusion, the study investigated two dose volume parameters, the gEUD and dose to volume, and their ability to connect to survival time. The analysis was able to produce multiple significant predictor dose cutoff values, that when applied to the patient group separated patients into decreased and increased survival groupings. However, the different patient populations suggested by the predictor groupings cannot be conclusively applied to one particular gEUD value or dose to volume value. Instead, the analysis offers potential areas for further investigation with larger patient populations and more robust methodologies.

BIBLIOGRAPHY

- [1] Python programming language official website. <http://www.python.org/>.
- [2] Research abstract program of the 2011 acvim forum denver, colorado, june 1518, 2011. Journal of Veterinary Internal Medicine, 25(3):632–767, 2011.
- [3] D.W. Andrews, C.B. Scott, P.W. Sperduto, A.E. Flanders, L.E. Gaspar, M.C. Schell, M. Werner-Wasik, W. Demas, J. Ryu, J.P. Bahary, et al. Whole brain radiation therapy with or without stereotactic radiosurgery boost for patients with one to three brain metastases: phase iii results of the rtog 9508 randomised trial. The Lancet, 363(9422):1665, 2004.
- [4] Stanley H Benedict, Kamil M Yenice, David Followill, James M Galvin, William Hinson, Brian Kavanagh, Paul Keall, Michael Lovelock, Sanford Meeks, Lech Papiez, Thomas Purdie, Ramaswamy Sadagopan, Michael C Schell, Bill Salter, David J Schlesinger, Almon S Shiu, Timothy Solberg, Danny Y Song, Volker Stieber, Robert Timmerman, Wolfgang A Tom, Dirk Verellen, Lu Wang, and Fang-Fang Yin. Stereotactic body radiation therapy: the report of AAPM task group 101. Medical Physics, 37(8):4078–4101, August 2010. PMID: 20879569.
- [5] S.M. Bentzen, L.S. Constine, J.O. Deasy, A. Eisbruch, A. Jackson, L.B. Marks, R.K. Ten Haken, and E.D. Yorke. Quantitative analyses of normal tissue effects in the clinic (quantec): an introduction to the scientific issues. International Journal of Radiation Oncology* Biology* Physics, 76(3):S3–S9, 2010.
- [6] D.J. Brenner. The linear-quadratic model is an appropriate methodology for determining isoeffective doses at large doses per fraction. In Seminars in radiation oncology, volume 18, pages 234–239. Elsevier, 2008.
- [7] C. Burman, GJ Kutcher, B. Emami, and M. Goitein. Fitting of normal tissue tolerance

- data to an analytic function. International Journal of Radiation Oncology* Biology* Physics, 21(1):123–135, 1991.
- [8] V. Ceder. The quick python book. Manning Publications Co., 2010.
- [9] B. Choi and J.O. Deasy. The generalized equivalent uniform dose function as a basis for intensity-modulated treatment planning. Physics in medicine and biology, 47:3579, 2002.
- [10] G. Cranmer-Sargison and S. Zavgorodni. Eud-based radiotherapy treatment plan evaluation: incorporating physical and monte carlo statistical dose uncertainties. Physics in medicine and biology, 50:4097, 2005.
- [11] J.A. de Pooter, W. Wunderink, A. Méndez Romero, P.R.M. Storchi, and B.J.M. Heijmen. Ptv dose prescription strategies for sbrt of metastatic liver tumours. Radiotherapy and Oncology, 85(2):260–266, 2007.
- [12] Joseph O Deasy, Andrzej Niemierko, Donald Herbert, Di Yan, Andrew Jackson, Randall K Ten Haken, Mark Langer, and Steve Sapareto. Methodological issues in radiation dose-volume outcome analyses: summary of a joint AAPM/NIH workshop. Medical Physics, 29(9):2109–2127, September 2002. PMID: 12349932.
- [13] P. Diaconis and B. Efron. Computer-intensive methods in statistics. Sci. Am.:(United States), 1983.
- [14] B. Emami, J. Lyman, A. Brown, L. Cola, M. Goitein, JE Munzenrider, B. Shank, LJ Solin, and M. Wesson. Tolerance of normal tissue to therapeutic irradiation. International Journal of Radiation Oncology Biology Physics, 21(1):109–122, 1991.
- [15] J.C. Flickinger, D. Kondziolka, A. Niranjan, and L.D. Lunsford. Results of acoustic neuroma radiosurgery: an analysis of 5 years’ experience using current methods. Journal of neurosurgery, 94(1):1–6, 2001.

- [16] H.A. Gay and A. Niemierko. A free program for calculating eud-based ntcp and tcp in external beam radiotherapy. Physica Medica, 23(3-4):115–125, 2007.
- [17] O. Gayou, D.S. Parda, and M. Miften. Euclid: An outcome analysis tool for high-dimensional clinical studies. Physics in medicine and biology, 52:1705, 2007.
- [18] J. Grimm, T. LaCouture, R. Croce, I. Yeo, Y. Zhu, and J. Xue. Dose tolerance limits and dose volume histogram evaluation for stereotactic body radiotherapy. Journal of Applied Clinical Medical Physics, 12(2), 2011.
- [19] J.A. Hanley. Characteristic (roc) curvel. Radiology, 743:29–36, 1982.
- [20] J. Harmon, D. Van Ufflen, and S. Larue. Assessment of a radiotherapy patient cranial immobilization device using daily on-board kilovoltage imaging. Veterinary Radiology & Ultrasound, 50(2):230–234, 2009.
- [21] D.P. Harrington and T.R. Fleming. A class of rank test procedures for censored survival data. Biometrika, 69(3):553–566, 1982.
- [22] P.J. Heagerty, T. Lumley, and M.S. Pepe. Time-dependent roc curves for censored survival data and a diagnostic marker. Biometrics, 56(2):337–344, 2000.
- [23] PJ Heagerty and P. Saha. survivalroc: Time-dependent roc curve estimation from censored survival data. R package, 1:0, 2006.
- [24] A.R. Henderson. The bootstrap: a technique for data-driven statistics. using computer-intensive analyses to explore experimental data. Clinica Chimica Acta, 359(1-2):1–26, 2005.
- [25] K. Jayasurya, G. Fung, S. Yu, C. Dehing-Oberije, D. De Ruyscher, A. Hope, W. De Neve, Y. Lievens, P. Lambin, and A. Dekker. Comparison of bayesian network and support vector machine models for two-year survival prediction in lung cancer patients treated with radiotherapy. Medical physics, 37:1401, 2010.

- [26] E. Jones, T. Oliphant, and P. Peterson. Scipy: Open source scientific tools for python. <http://www.scipy.org/>, 2001.
- [27] B D Kavanagh, R D Timmerman, S H Benedict, Q Wu, T E Schefter, K Stuhr, S McCourt, F Newman, R M Cardinale, and L F Gaspar. How should we describe the radiobiologic effect of extracranial stereotactic radiosurgery: equivalent uniform dose or tumor control probability? Medical Physics, 30(3):321–324, March 2003. PMID: 12674231.
- [28] Brian D Kavanagh, Moyed Miften, and Rachel A Rabinovitch. Advances in treatment techniques: stereotactic body radiation therapy and the spread of hypofractionation. Cancer Journal (Sudbury, Mass.), 17(3):177–181, June 2011. PMID: 21610471.
- [29] H.P. Langtangen. Python scripting for computational science, volume 3. Springer Verlag, 2006.
- [30] H.P. Langtangen. A Primer on Scientific Programming with Python, volume 6. Springer Verlag, 2009.
- [31] X.A. Lib, M. Alber, J.O. Deasy, A. Jackson, K.W.K. Jee, L.B. Marks, M.K. Martel, C. Mayo, V. Moiseenko, A.E. Nahum, et al. The use and qa of biologically related models for treatment planning: Short report of the tg-166 of the therapy physics committee of the aapm. Medical Physics, 39(3), 2012.
- [32] L.B. Marks, EJ Hall, and DJ Brenner. Extrapolating hypofractionated radiation schemes from radiosurgery data: Regarding hall et al., ijrobp 21: 819-824; 1991 and hall and brenner, ijrobp 25: 381-385; 1993. authors’response. International journal of radiation oncology, biology, physics, 32(1):274–276, 1995.
- [33] A Martin and A Gaya. Stereotactic body radiotherapy: a review. Clinical Oncology (Royal College of Radiologists (Great Britain)), 22(3):157–172, April 2010. PMID: 20092981.

- [34] A. Niemierko. Reporting and analyzing dose distributions: a concept of equivalent uniform dose. Medical Physics, 24:103, 1997.
- [35] A. Niemierko. A generalized concept of equivalent uniform dose (eud). Med Phys, 26(6):1100, 1999.
- [36] Clint Park, Lech Papiez, Shichuan Zhang, Michael Story, and Robert D Timmerman. Universal survival curve and single fraction equivalent dose: useful tools in understanding potency of ablative radiotherapy. International Journal of Radiation Oncology, Biology, Physics, 70(3):847–852, March 2008. PMID: 18262098.
- [37] Kyle E Rusthoven, Brian D Kavanagh, Higinia Cardenes, Volker W Stieber, Stuart H Burri, Steven J Feigenberg, Mark A Chidel, Thomas J Pugh, Wilbur Franklin, Madeleine Kane, Laurie E Gaspar, and Tracey E Schefter. Multi-institutional phase I/II trial of stereotactic body radiation therapy for liver metastases. Journal of Clinical Oncology: Official Journal of the American Society of Clinical Oncology, 27(10):1572–1578, April 2009. PMID: 19255321.
- [38] Tracey E Schefter, Brian D Kavanagh, Robert D Timmerman, Higinia R Cardenes, Anna Baron, and Laurie E Gaspar. A phase i trial of stereotactic body radiation therapy (SBRT) for liver metastases. International Journal of Radiation Oncology, Biology, Physics, 62(5):1371–1378, August 2005. PMID: 16029795.
- [39] S.L. Stafford, B.E. Pollock, R.L. Foote, M.J. Link, D.A. Gorman, P.J. Schomberg, and J.A. Leavitt. Meningioma radiosurgery: tumor control, outcomes, and complications among 190 consecutive patients. Neurosurgery, 49(5):1029, 2001.
- [40] C. Thieke, T. Bortfeld, A. Niemierko, and S. Nill. From physical dose constraints to equivalent uniform dose constraints in inverse radiotherapy planning. Medical physics, 30:2332, 2003.

- [41] Emma Thomas, Olivier Chapet, Marc L Kessler, Theodore S Lawrence, and Randall K Ten Haken. Benefit of using biologic parameters (EUD and NTCP) in IMRT optimization for treatment of intrahepatic tumors. International Journal of Radiation Oncology, Biology, Physics, 62(2):571–578, June 2005. PMID: 15890602.
- [42] R.D. Timmerman. An overview of hypofractionation and introduction to this issue of seminars in radiation oncology. In Seminars in radiation oncology, volume 18, page 215, 2008.
- [43] Jian Z Wang and X Allen Li. Evaluation of external beam radiotherapy and brachytherapy for localized prostate cancer using equivalent uniform dose. Medical Physics, 30(1):34–40, January 2003. PMID: 12557976.
- [44] S.J. Withrow and D.M. Vail. Withrow & MacEwen’s small animal clinical oncology. Saunders Elsevier St Louis, 2007.
- [45] Q. Wu, R. Mohan, A. Niemierko, and R. Schmidt-Ullrich. Optimization of intensity-modulated radiotherapy plans based on the equivalent uniform dose. International Journal of Radiation Oncology Biology Physics, 52(1):224–235, 2002.